

# Subsolidus phase relations, crystal chemistry and cation-transport properties of sodium iron antimony oxides

V.V. Politaev, V.B. Nalbandyan\*

Chemistry Faculty, South Federal University, ul. Zorge 7, 344090 Rostov-na-Donu, Russia

Received 7 February 2008; received in revised form 27 March 2008; accepted 11 April 2008

Available online 25 April 2008

## Abstract

Subsolidus phase relations in  $\text{Na}_2\text{O}-\text{Fe}_2\text{O}_3-\text{Sb}_2\text{O}_x$  system (excluding Na-rich and Sb-rich corners) were studied using powder X-ray diffraction. Samples were prepared by conventional solid-state reactions at 980–1030 °C followed by quenching. Sb substitution for Fe stabilizes the low-temperature rhombohedral  $\alpha$  form of  $\text{NaFeO}_2$  and enhances ionic conductivity:  $\sigma(300\text{ °C}) = 0.5\text{ S/m}$ ,  $E_a = 0.38(3)\text{ eV}$ ,  $t_e < 0.01$  for  $\text{Na}_{0.8}\text{Fe}_{0.9}\text{Sb}_{0.1}\text{O}_2$  ceramics. Besides known orthorhombic  $\text{Na}_2\text{Fe}_3\text{SbO}_8$ , three new compounds have been identified: trigonal  $\text{Na}_4\text{FeSbO}_6$ , a superlattice of  $\alpha$ - $\text{NaFeO}_2$  type,  $a = 5.4217(7)\text{ \AA}$ ,  $c = 16.2715(1)\text{ \AA}$ , possible space group  $P3_112$ ; orthorhombic  $\text{Na}_2\text{FeSbO}_5$ , possibly related to brownmillerite,  $Pbcn$ ,  $a = 10.8965(13)\text{ \AA}$ ,  $b = 15.7178(13)\text{ \AA}$ ,  $c = 5.3253(4)\text{ \AA}$ , and one more phase with empirical formula  $\text{Na}_4\text{Fe}_3\text{SbO}_9$ , whose pattern could not be indexed. Ion-exchange reactions lead to a delafossite-type superlattice  $\text{Ag}_3(\text{NaFeSb})\text{O}_6$  ( $a = 5.4503(12)\text{ \AA}$ ,  $c = 18.7747(20)\text{ \AA}$ , possible space group  $P3_112$ ).

© 2008 Elsevier Masson SAS. All rights reserved.

**Keywords:** Antimonate; Ionic conductivity; Ion exchange; X-ray diffraction;  $\alpha$ - $\text{NaFeO}_2$  type; Superlattice; Ceramics

## 1. Introduction

Recently [1–3], a series of quasi-ternary systems  $\text{A}_2\text{O}-\text{MO}-\text{Sb}_2\text{O}_5$  (where  $\text{A} = \text{Na}$  or  $\text{K}$ ,  $\text{M} = \text{Co}$ ,  $\text{Ni}$ ,  $\text{Cu}$ ,  $\text{Zn}$ , or  $\text{Mg}$ ) was investigated and several non-stoichiometric layered phases,  $\text{A}_x\text{M}_{(1+x)/3}\text{Sb}_{(2-x)/3}\text{O}_2$  were found. Some of them exhibit considerable cationic conductivity. In their structures,  $\text{M}^{2+}$  and  $\text{Sb}^{5+}$  are distributed at random over octahedral sites within brucite-like  $(\text{M,Sb})\text{O}_{6/3}$  layers. However, ordered phases appeared at the sodium-containing stoichiometric compositions,  $x = 1$ , i.e.,  $\text{Na}_3\text{M}_2\text{SbO}_6$ . Preliminary results on some sodium iron antimony oxides were also reported [1]. In continuation of these studies, we report here more detailed data on the  $\text{Na}_2\text{O}-\text{Fe}_2\text{O}_3-\text{Sb}_2\text{O}_5$  system.

To our knowledge, this quasi-ternary system was not studied in detail previously. However, one ternary oxide,  $\text{Na}_2\text{Fe}_3\text{SbO}_8$ , was identified [4]. Here, again,  $\text{Sb}^{5+}$  substitutes for  $\text{Fe}^{3+}$  on

octahedral sites of  $\text{CaFe}_2\text{O}_4$ -type structure. According to diffraction data, the substitution is random, but IR spectra indicate a tendency to local ordering. In the  $\text{Na}_2\text{O}-\text{Sb}_2\text{O}_5$  quasi-binary system, three sodium antimonates (5+) are known: monoclinic  $\text{Na}_3\text{SbO}_4$  [5], rhombohedral ilmenite-type  $\text{NaSbO}_3$  [6] and orthorhombic  $\text{NaSb}_5\text{O}_{13}$  [7]. However,  $\text{NaSb}_5\text{O}_{13}$ , prepared by the hydrothermal method, is unstable at high temperatures. Partial reduction takes place in the antimony-rich region, and the system transforms into a ternary one,  $\text{Na}_2\text{O}-\text{Sb}_2\text{O}_5-\text{Sb}_2\text{O}_3$ . Cubic pyrochlore-type phase,  $\text{Na}_{1+x}\text{Sb}_{1-x}^{3+}\text{Sb}_2^{5+}\text{O}_{7-x}$ , is homogeneous between ca. 25 and 37 mol%  $\text{Na}_2\text{O}$  at 800–1300 °C [8,9], and  $\text{Sb}_2\text{O}_4$  (rather than  $\text{NaSb}_5\text{O}_{13}$ ) appears at lower alkali content. Only one compound,  $\text{FeSbO}_4$ , exists in the  $\text{Fe}_2\text{O}_3-\text{Sb}_2\text{O}_5$  system [10]. According to X-ray diffraction data, it has disordered rutile type structure, but electron diffraction [11] and density functional calculations [12] indicate ordering of  $\text{Fe}^{3+}$  and  $\text{Sb}^{5+}$  on octahedral sites. In the  $\text{Na}_2\text{O}-\text{Fe}_2\text{O}_3$  system, monoclinic  $\text{Na}_3\text{Fe}_5\text{O}_9$  [13] and trimorphic  $\text{NaFeO}_2$  [14] are known, as well as several alkali-rich compounds ( $\text{Na/Fe} > 1$ ) which are out of the scope of present work. Low-temperature  $\alpha$ - $\text{NaFeO}_2$  contains all the

\* Corresponding author. Tel.: +7 8632975145.

E-mail address: [vbn@rsu.ru](mailto:vbn@rsu.ru) (V.B. Nalbandyan).

ions in distorted octahedral coordination, whereas they are coordinated tetrahedrally in both high-temperature forms,  $\beta$  and  $\gamma$ .

## 2. Experimental

All samples were prepared by conventional solid-state reactions. Reagent-grade sodium carbonate, antimonous acid  $\text{Sb}_2\text{O}_3 \cdot x\text{H}_2\text{O}$ , ferric oxide and hydrous ferric nitrate were used as starting materials.  $\text{Na}_2\text{CO}_3$  and  $\text{Fe}_2\text{O}_3$  were dried before using; antimonous acid and ferric nitrate were analysed by calcining at  $850^\circ$  to give  $\text{Sb}_2\text{O}_4$  and  $\text{Fe}_2\text{O}_3$ , respectively, and used for syntheses in the air-dry form. To facilitate homogenizing Fe and Sb cations,  $\text{FeSbO}_4$  was prepared first. Ferric nitrate and antimonous acid were mixed and heated slowly, with intermediate regrindings, to  $600^\circ\text{C}$ , then pressed and calcined at  $1050^\circ\text{C}$  for 3 h. X-ray diffraction (XRD) indicated pure phase. Ternary compositions were prepared from  $\text{FeSbO}_4$ ,  $\text{Na}_2\text{CO}_3$  and  $\text{Fe}_2\text{O}_3$  (or antimonous acid). Weighed amounts of powders (2–4 g total mass) were thoroughly mixed with a mortar and pestle, pressed into pellets, calcined at  $750^\circ\text{C}$  to remove volatile components, reground, pressed, fired at  $980$ – $1030^\circ\text{C}$  for 2–3 h and quenched onto a massive steel plate to prevent phase changes. In some preparations, ferric nitrate was used instead of the oxide, and the heat treatments started from lower temperatures.

Repeated firings showed gradual depletion in sodium oxide due to its volatility. To compensate for this, an empirically chosen sodium excess (2–3% of the calculated amount) was introduced, and the pellets were covered with the powder of the same composition. XRD phase analysis was performed using a DRON 2.0 diffractometer with Ni-filtered  $\text{Cu K}_\alpha$  radiation, and the high-temperature treatment was repeated to ensure that equilibrium was attained. For some single-phase samples, XRD data were collected with a Rigaku D/Max-B or Geigerflex D/Max-RC instrument equipped with a secondary-beam curved graphite monochromator using  $\text{Cu K}_\alpha$  radiation and submitted to the Powder Diffraction File (# 00-053-351, 00-054-888, 00-055-705, 00-057-673). Corundum powder (NIST SRM 676) served as  $2\theta$  standard. Indexing was performed by analogy with similar phases or using the ITO program [15], cell constants were refined by CELREF3 (Laugier and Bochu, 2001).

Ceramic samples for the conductivity measurements were prepared from pre-calcined powders by uniaxial hot pressing at 40 MPa,  $980^\circ\text{C}$ . A cylindrical green compact was placed into a hot-pressing die and surrounded with coarse-grained alumina to ensure the quasi-hydrostatic regime. After pressing, rectangular samples were cut, polished and electroded with molten indium. Only single-phase ceramics, characterized by XRD prior to the electrical measurements, was used for the impedance spectroscopy studies carried out in the frequency range 20 Hz–200 KHz using a P5021 bridge. To estimate electronic conductivity (without discrimination between n- and p-type), dc polarization method was used with a constant voltage of 100 mV. For ion-exchange experiments, the powders were mixed with 10–20% excess silver nitrate, reacted for an hour at  $240^\circ\text{C}$  (i.e., slightly above the melting

point of  $\text{AgNO}_3$ ) and washed with water. Silver content in the products was determined by titration with thiocyanate after dissolving in hot concentrated  $\text{H}_2\text{SO}_4$  and dilution.

## 3. Results and discussion

### 3.1. Subsolidus phase relation in the $\text{Na}_2\text{O}$ – $\text{Fe}_2\text{O}_3$ – $\text{Sb}_2\text{O}_5$ system

As indicated above, reduction to  $\text{Sb}^{3+}$  occurs in the antimony-rich region, whereas preparation of alkali-rich samples is difficult due to high volatility of sodium oxide at elevated temperatures and relatively low melting point of sodium carbonate. Hence, Na-rich and Sb-rich corners were excluded, and the investigated composition range was confined to the  $\text{NaSb}_3\text{O}_7$ – $\text{Na}_3\text{SbO}_4$ – $\text{NaFeO}_2$ – $\text{Fe}_2\text{O}_3$ – $\text{FeSbO}_4$  pentagon. In this region, 40 different compositions were prepared and examined. Their powder patterns did not change on repeated firings, and at most three phases were found in each sample. These results indicate equilibrium attained at  $980^\circ\text{C}$  and enable partition of the system into phase compatibility triangles (Fig. 1). Preparing the single-phase ternary oxides was somewhat more difficult and needed additional heat treatments at  $1000$ – $1030^\circ\text{C}$ . Five ternary oxides, of which only one was known from the literature [4], were identified in the system and marked A, B, C, D and X in Fig. 1. The compositions of A, B, C, and D were established to within ca. 1 mol% and converted into empirical formulas listed in Table 1 together with the crystallographic data. With the phase X, the phase analysis is complicated, as discussed below. Powder patterns for the new phases are shown in Figs 2 and 3.

### 3.2. Phase A, $\text{Na}_{1-x}\text{Fe}_{1-x/2}\text{Sb}_{x/2}\text{O}_2$

On the isothermal section (Fig. 1), this phase seems to be an individual non-stoichiometric compound, but its powder

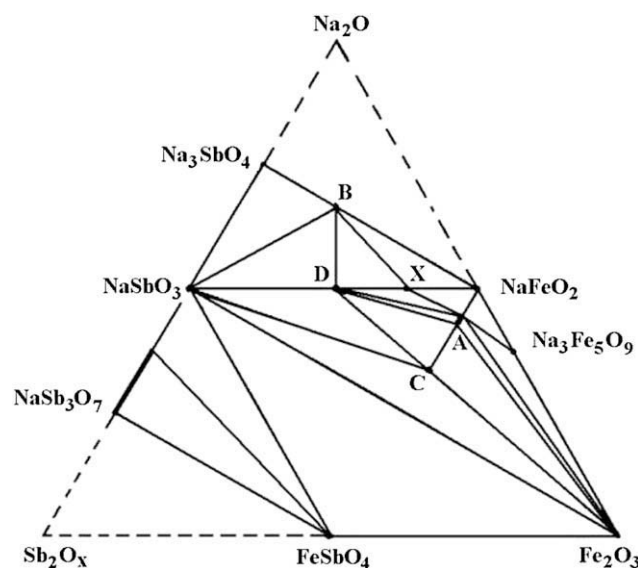


Fig. 1. Phase compatibility diagram of the  $\text{Na}_2\text{O}$ – $\text{Fe}_2\text{O}_3$ – $\text{Sb}_2\text{O}_x$  system at  $980^\circ\text{C}$  in air. For designation of phases A, B, C, D, and X, see Table 1 and the text.

Download English Version:

<https://daneshyari.com/en/article/1506103>

Download Persian Version:

<https://daneshyari.com/article/1506103>

[Daneshyari.com](https://daneshyari.com)